Available online at www.sciencedirect.com
SCIENCE DIRECT®

GEOTHERMICS

Geothermics 34 (2005) 568–591

www.elsevier.com/locate/geothermics

Hydrology and reservoir characteristics of three geothermal systems in western Uganda☆

Godfrey Bahati[a], Zhonghe Pang[b,*], Halldór Ármannsson[c], Edward M. Isabirye[a], Vicent Kato[a]

[a] Department of Geological Survey and Mines, P.O Box 9, Entebbe, Uganda
[b] International Atomic Energy Agency, Vienna, Austria
[c] Icelandic Geosurvey, Grensasvegur 9, 108 Reykjavik, Iceland

Received 21 January 2005; accepted 28 June 2005

Abstract

Several sampling surveys have been carried out in three geothermal areas in western Uganda, known as Katwe-Kikorongo (Katwe), Buranga, and Kibiro. Sixty-three water samples from hot and cold springs, dug wells, rivers, and lakes, and 14 rock samples from surface outcrops have been collected and analyzed. They were then analyzed for chemistry and isotopes of hydrogen ($\delta^2H_{H_2O}$, $^3H_{H_2O}$), oxygen ($\delta^{18}O_{H_2O}$, $^{18}O_{SO_4}$), carbon ($\delta^{13}C_{DIC}$, $^{14}C_{DIC}$), sulfur ($\delta^{34}S_{SO_4}$), and strontium ($^{87/86}Sr_{H_2O}$, $^{87/86}Sr_{Rock}$). The results suggest a meteoric origin for the geothermal waters, with little secondary alteration. Based on isotope data, Katwe and Buranga are recharged from the Rwenzori Mountains, and Kibiro from high ground represented by the Mukihani-Waisembe Ridge in Kitoba Sub-county, 20 km to the southeast. Oxygen isotope geothermometry, based on aqueous sulfate and water equilibrium fractionation, indicates a subsurface temperature of 200 °C for Buranga, which is higher than that inferred from chemical geothermometry (160–170 °C), and lower temperatures (140–150 °C) for Katwe and Kibiro that are similar to the results of chemical geothermometry. Tritium concentrations indicate some involvement of modern cold water close to the surface at Kibiro but not at Buranga and Katwe, where hot springs discharge tritium-free waters. Sulfur isotope ratios ($\delta^{34}S_{SO_4}$) of hot water suggest magmatic contributions of sulfate in all three areas, confirming the results of earlier

☆ This paper is the sixth of a set of articles describing the use of isotope and hydrochemical methods in geothermal R&D, published in Vol. 34, No. 4 and guest-edited by Zhonghe Pang and Alfred Truesdell.

* Corresponding author. Present address: Institute of Geology and Geophysics, Chinese Academy of Sciences, P.O. Box 9825, Beijing 100029, China. Fax: +86 10 6201 0846.
E-mail address: z.pang@mail.iggcas.ac.cn (Z. Pang).

doi:10.1016/j.geothermics.2005.06.005

geochemical investigations. Strontium isotope ratios in water and rock samples ($^{87/86}Sr_{H_2O}$, $^{87/86}Sr_{Rock}$) allow a preliminary identification of rock types that may have interacted with the thermal waters.

Keywords: Isotopes; Recharge; Geothermometry; Salinity; Katwe-Kikorongo; Buranga; Kibiro; Uganda

1. Introduction

The geological and geotectonic setting of the East Africa Rift System (EARS) suggests that it is very promising for geothermal development. Some areas, particularly in the eastern branch of the EARS in Kenya and Ethiopia, are already being exploited or are under exploration. In the western branch of the EARS, however, thorough exploration has proceeded rather slowly, partly because of a limited scientific understanding of the geothermal systems.

Uganda is one of the East African countries traversed by the western branch of the EARS, and, based on surface manifestations, its potential for geothermal energy development is high. For more than a decade, the Ugandan government has supported a geothermal development programme to provide electricity or direct heat to rural areas for domestic power, industrial processing and engineered agriculture.

The results of the 1999–2003 isotope hydrology project supported by the International Atomic Energy Agency are presented here. The three most promising geothermal prospects in Uganda (Katwe-Kikorongo (Katwe), Buranga and Kibiro), located along the Congolese border (Fig. 1) in the Western Rift Valley, have been investigated. The main objectives of this study were to: (1) elucidate the origin of the geothermal fluids, (2) identify the recharge mechanisms, (3) estimate subsurface temperature using isotope geothermometry, (4) trace the source of solutes, and (5) improve the conceptual geothermal models of the study areas.

2. Geology and hydrogeology

2.1. Climate

Uganda straddles the Equator, covering an area of approximately 241,000 km^2, of which 15.3% is open water and 12.4% wetlands. The climate can be categorised as tropical with both wet and dry seasons, but sub-climatic zones exist and are differentiated mainly by altitude and rainfall. Rainfall exhibits a yearly bimodal distribution with two peaks, in March–May and September–November. The highest annual rainfall, of around 2000 mm, is recorded for areas around Lake Victoria, while the lowest (about 600 mm) is recorded in the northern and eastern parts of the country. The average annual precipitation for Uganda is estimated to be 1200 mm. The average annual potential evapotranspiration is 1400 mm and exceeds precipitation during most of the year. Mean temperatures over the entire country fluctuate widely, depending on elevation and landscape, and vary between 18 and 33 °C throughout the year.

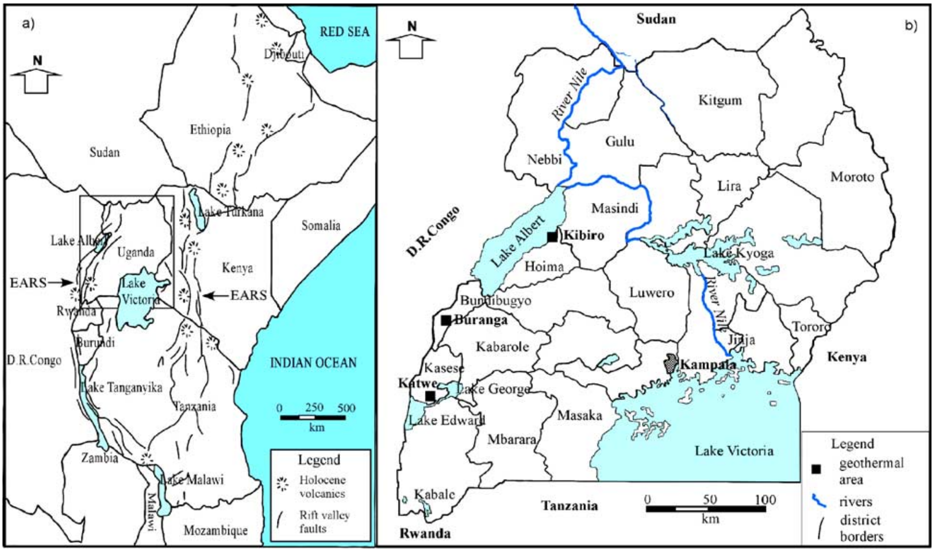

Fig. 1. (a) The East African Rift System (EARS) and (b) location of the three main geothermal areas in Uganda (Katwe, Buranga and Kibiro). D.R.C., Democratic Republic of Congo.

The climate in Katwe and Buranga areas is influenced by the Rwenzori Mountains to the north and east, respectively. These mountains are a massif block that is believed to have been uplifted during the Tertiary period; they are hidden in a cloud cover created periodically by moist air streams from the Atlantic and Indian Oceans. The tops of the Rwenzori Mountains are covered by permanent ice and snow, with a total of 37 small glaciers and ice fields covering about 67 km^2. The mean annual rainfall reaches up to 2000 mm at an altitude of about 4600 m above sea level.

The Katwe geothermal area lies at the foot of the Rwenzori Mountains. This location, at an elevation of approximately 900 m in the rain shadow of the towering mountains, is hot and dry, with a mean annual rainfall of the order of 800–1000 mm, and a mean annual temperature of about 27 °C. At higher altitude, the mean annual rainfall may exceed 1800 mm, while barely 10–30 km away in the Rift Valley the corresponding rainfall is less than 800 mm (EASD, 1996). The Katwe area is characterized by low precipitation and high rates of evaporation with much reduced surface flow. On the whole, evaporation exceeds precipitation.

Buranga is also located at the foot of the Rwenzori Mountains and is generally humid and characterized by excess moisture because precipitation is much higher locally than evapo-transpiration. There is potential for groundwater recharge from snowmelt run-off, small lakes in the upper valleys of the Rwenzori Mountains, as well as local precipitation.

The Kibiro geothermal area is located further north, under the escarpment of the Rift Valley on the shores of Lake Albert. It is hot and dry almost all year and lies in the rain shadow of the mountains, so there is little rainfall. On the plateau east of the Rift, annual rainfall is considerably higher than in the Rift itself.

2.2. Regional geology

The geology of Uganda consists of an exposed Precambrian basement dissected by the western branch of the EARS in the western part of the country. The eastern branch, the Gregory Rift, passes through the central part of Kenya. The Western Rift starts to the north along the Sudan border, and then curves to the west, southwest along the border with the Democratic Republic of Congo, and south to Rwanda and Burundi. Spreading began at least 15 million years ago in Miocene time.

The Western Rift, where the Katwe, Buranga and Kibiro geothermal areas are located, is considered at an early stage of development, and is younger (late Miocene–Recent) than the more mature eastern branch (Morley and Westcott, 1999). The region of the Rift has a markedly higher heat flow than the surrounding Precambrian terrain. Two different en-echelon folding strands are found in the Western Rift, separated by the Rwenzori Mountains, which rise from less than 1000 m in the Rift Valley to over 5000 m elevation. Within the valley there are thick layers of late Tertiary and Quaternary sediments, fresh water and saline crater lakes; volcanic rocks and plutonic bodies have been identified beneath Lakes Albert and Edward (EDICON, 1984) (Fig. 2).

2.3. Geology of Katwe-Kikorongo and surrounding areas

The Katwe-Kikorongo volcanic field covers approximately 200 km^2 (Fig. 3) within which lies the Katwe geothermal area. There are a large number of craters most of which lie on the main fault, striking NE-SW. The geology is characterized by explosion craters and ejected pyroclastics and tuffs, with abundant basement granite and gneissic rocks. Minor occurrences of lava are found mainly in the Kitagata and Kyemengo crater areas. The age of the volcanic activity has been estimated at Pleistocene to Holocene (Musisi, 1991). The volcanoes rise gently to a maximum of 300–400 m above the Rift Valley. The sediments in the valley are grayish, generally coarse-grained and calcareous sands.

Geothermal surface manifestations are relatively scarce, and found in two craters only, Katwe and Kitagata, both of which are host crater lakes. Lake Katwe lies on the floor of an explosion crater formed in tuffs, with only 200–250 m of rock separating it from Lake Edward at the closest point. Hydrological and geophysical investigations indicate that there is no hydrological connection between the two lakes despite Lake Edward being 30 m higher in elevation than Lake Katwe. A few springs with slightly above ambient temperatures emerge near Katwe crater lake. At Lake Kitagata there are five hot springs, one at the bottom of this crater lake. No mineral precipitation or hydrothermal alteration is evident, but the temperatures range between 56 and 70 °C.

Recharge by infiltrating meteoric waters is likely along major fracture (i.e. permeable) zones, both along the roughly circular perimeter of the volcano-tectonic depression and transverse to it. The bases of lava flows are also likely to provide migration pathways. The crater lakes are hydrologically isolated from the fresh water Lakes Edward and George, despite being at lower or similar elevations, which gives some indication of the complexity of the local hydrogeologic system.

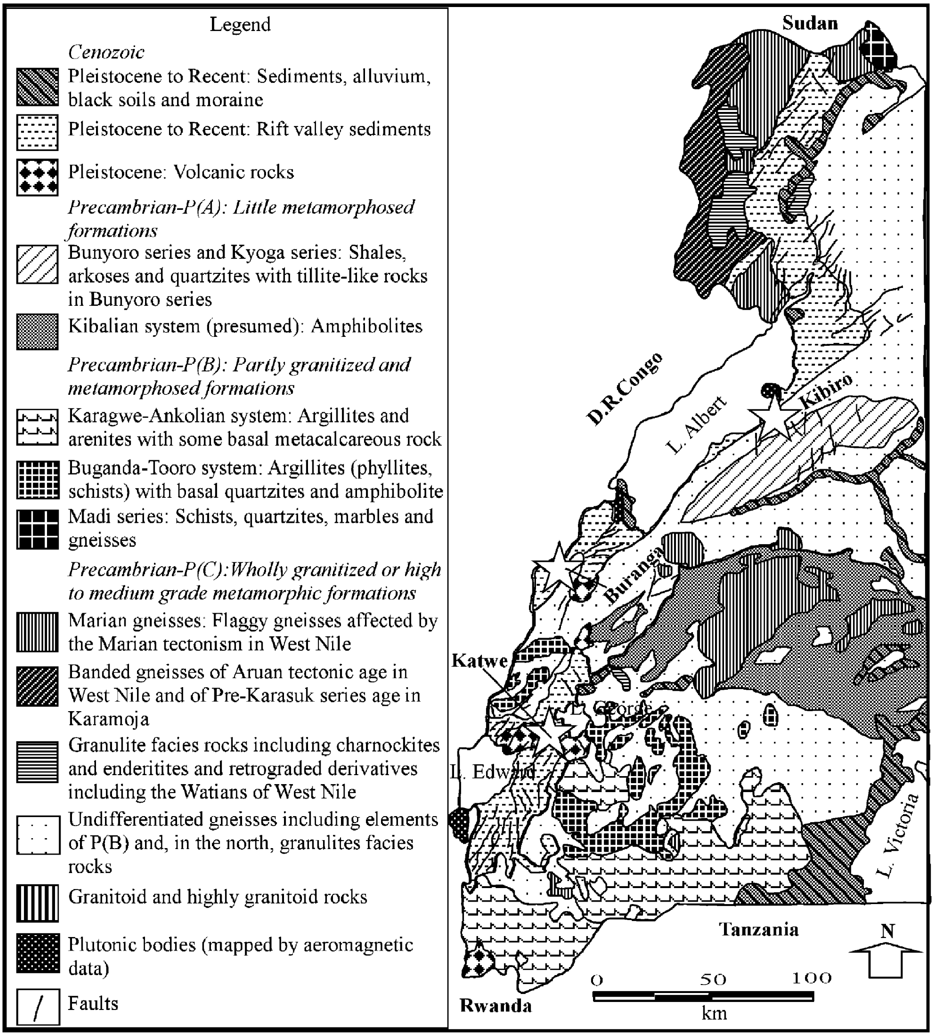

Fig. 2. Geology of the Western Rift Valley in Uganda. D.R.C., Democratic Republic of Congo.

2.4. Geology of Buranga and surroundings

The Buranga geothermal area is located at the northwestern end of the Rwenzori Mountains in the Western Rift Valley (Fig. 4). Unlike Katwe, Buranga shows no evidence of volcanism but is highly active tectonically. Geothermal surface activity is intense, with spouting hot springs and high gas flow. The manifestations occur at the foot of the eastern escarpments in a swampy area within a dense rain forest. Surface alteration is scarce but many of the springs have developed terraces and mounts of travertine deposits.

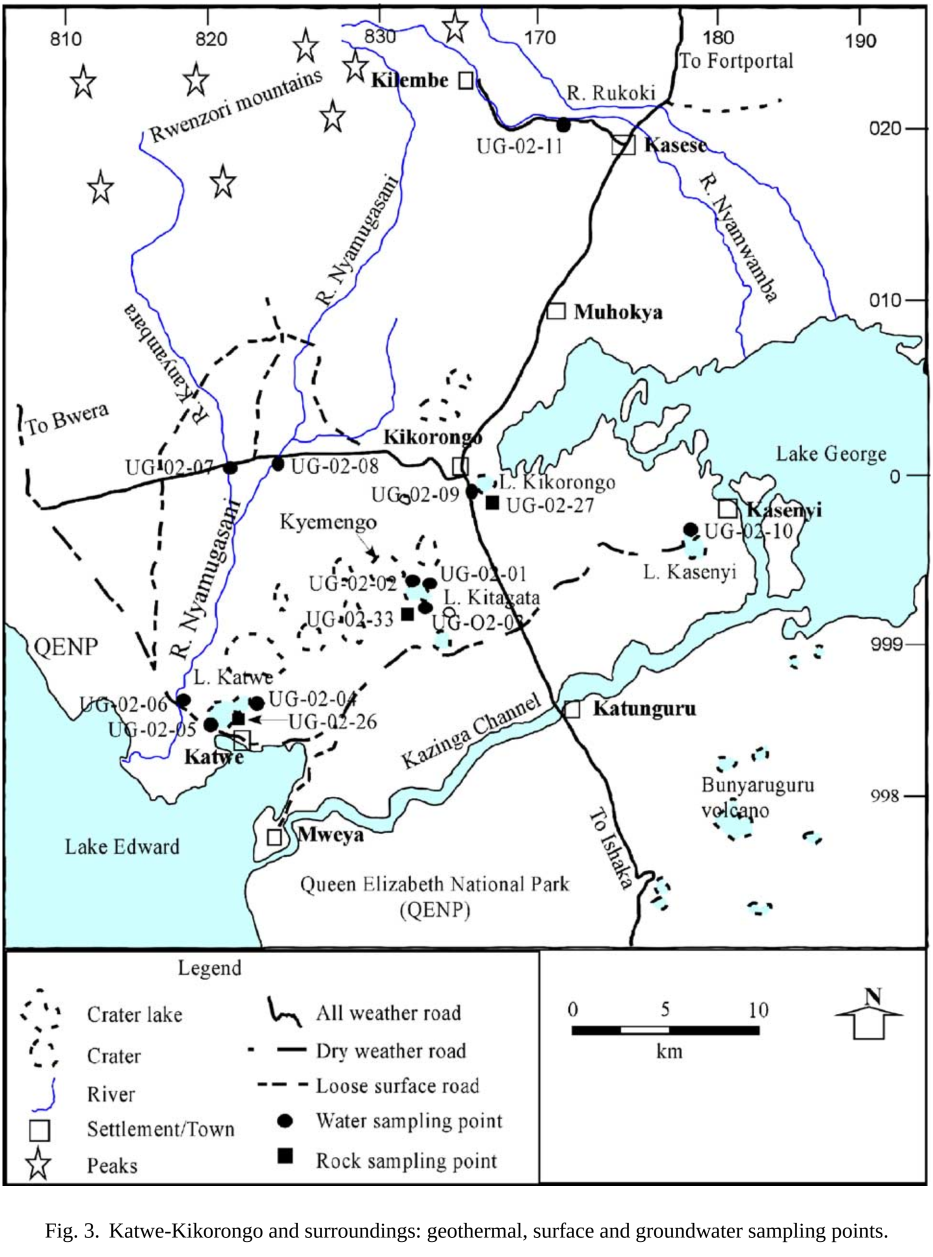

Fig. 3. Katwe-Kikorongo and surroundings: geothermal, surface and groundwater sampling points.

Recent surface and geological observations indicate the presence of extinct thermal features (travertine deposits) along a zone stretching for 10 km north of the Buranga hot springs. This indicates that the area of thermal activity has been shifting from north to south and that the underground geothermal activity in Buranga area may be somewhat larger than indicated by the present-day surface manifestations.

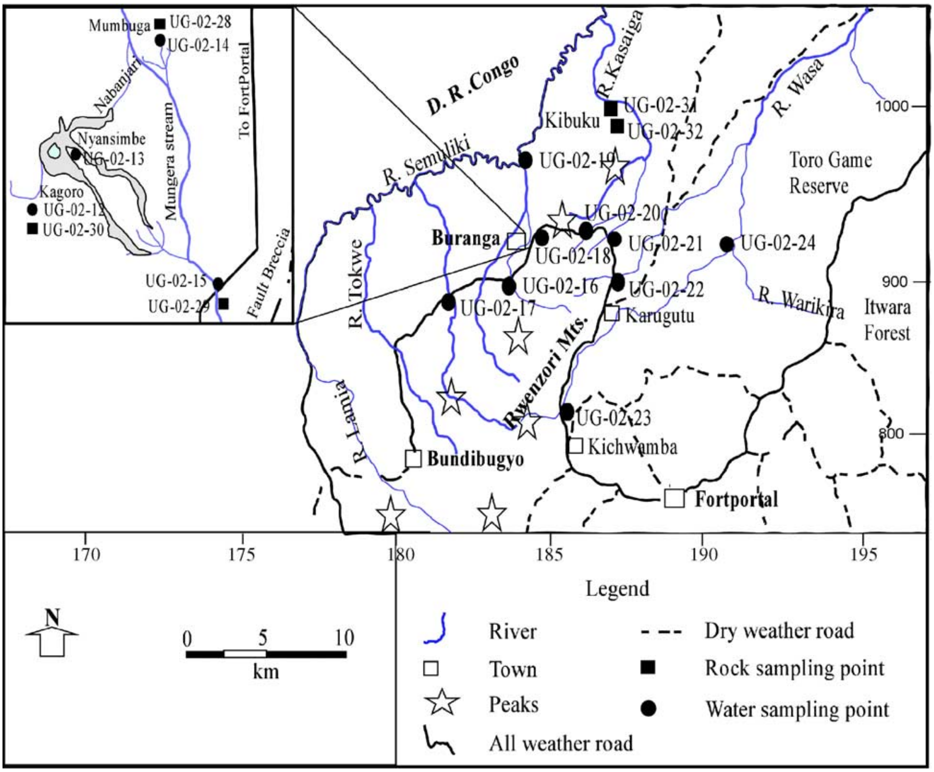

Fig. 4. Buranga and surroundings: geothermal, surface and groundwater sampling points.

2.5. Geology of Kibiro geothermal area

The Kibiro geothermal area is located on the shores of Lake Albert on the eastern escarpment front of the Western Rift Valley (Fig. 5).

The escarpment, which cuts through the field from SW to NE, divides the study area into two entirely different geological environments. To the east, the geology is dominated by an ancient crystalline basement, characterized by granites and granitic gneisses, whereas in the Rift Valley to the west there are sequences of sediments, at least 5.5 km thick, without any volcanic rocks at the surface. The Kibiro hot springs emerge in the sediments at the foot of the escarpment.

The Albertine Rift, as part of the Western Rift, is seismically active, characterized by large, deep-seated (27–40 km) earthquakes.

The Kibiro hot springs are characterised by the presence of H_2S and white thread-like algae, some of which are coloured black with sulfides. On the lower slopes of the fault escarpment south-west of the springs, sulfur deposits on the brecciated outcrops and sulfur crystal growth in cracks have been identified and mapped. No steam has been seen rising, but the smell and fresh deposits of sulfur indicate that some H_2S is being released. Recent

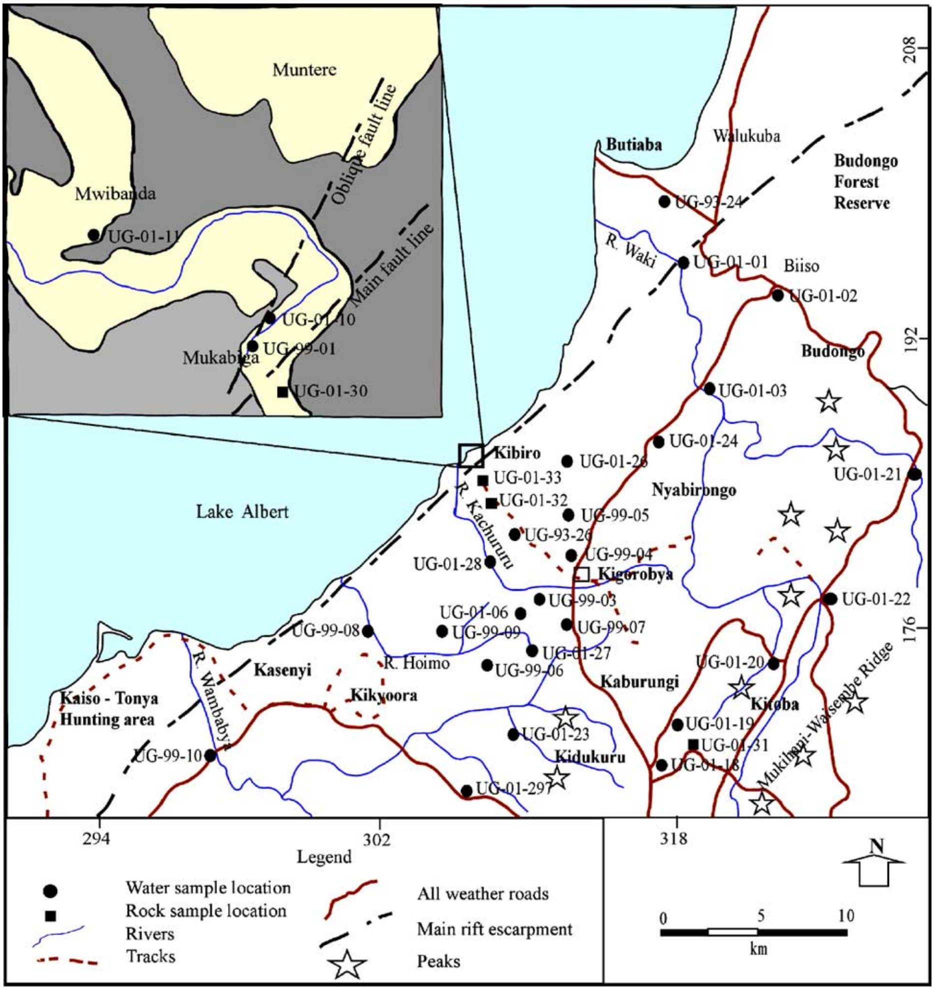

Fig. 5. Kibiro and surroundings: geothermal, surface and groundwater sampling points.

geological and geophysical studies show that the geothermal resource can be traced along faults within the block-faulted granites to the east away from the Rift. Low resistivity (<5 Ωm) is associated with the fault lines, and calcite deposits are common. A gravity high observed in the granites may indicate intrusives, and dike-like intrusives have been identified (Gíslason et al., 2004).

3. Sampling and analyses

A total of 63 water samples from hot and cold springs, dug wells, rivers and lakes, as well as 14 samples from surface outcrops of different types of rocks, were collected and analyzed for chemical and isotopic compositions. Isotopes analyzed included hydrogen ($\delta^2H_{H_2O}$, $^3H_{H_2O}$), oxygen ($\delta^{18}O_{H_2O}$, $^{18}O_{SO_4}$), carbon ($\delta^{13}C_{DIC}$, $^{14}C_{DIC}$), sulfur ($\delta^{34}S_{SO_4}$), and strontium ($^{87/86}Sr_{H_2O}$, $^{87/86}Sr_{Rock}$), where DIC represents dissolved inorganic carbon. Field measurements of temperature, pH, and electrical conductivity, and analysis of volatiles (CO_2 and H_2S) etc., were carried out on site. The sampling points are shown in Figs. 3–5 for Katwe-Kikorongo, Buranga and Kibiro, respectively.

Chemical and isotope analyses of water and rock samples were carried out at the IAEA isotope hydrology laboratory in Vienna, Austria, at the Institute of Hydrology in Munich, Germany (S-34) and at the Institute of Geosciences and Earth Resources (Sr-87) in Pisa, Italy.

Cations were analyzed using Inductively Coupled Plasma (ICP) methods and anions were analyzed by ion chromatography. Aqueous sulfate was collected by precipitation as $BaSO_4$ after acidification. The precipitate was then reacted with graphite to produce CO_2 for mass spectrometer measurement of $\delta^{18}O_{SO_4}$. Sulfur dioxide (SO_2) for mass spectrometry of $\delta^{34}S$ was prepared by oxidizing precipitated BaS. In most water samples, Sr concentrations were measured by Atomic Absorption Spectrometer. Uncertainties in concentration range from 5 to 15% for the more complex samples. For strontium isotopes, ten internal standards (NIST 987) were measured together with the samples in order to correct for any isotopic fractionation occurring in the chemical preparation and mass spectrometric measurements.

Data handling and interpretation were carried out at the IAEA headquarters in Vienna jointly by technical staff of the IAEA and their Ugandan counterparts.

4. Results and discussions

Details of sites and dates for samples from Kibiro, and from Katwe-Kikorongo and Buranga are shown in Tables 1 and 2, respectively. Results of chemical analysis are given in Tables 3 and 4 for Kibiro and Katwe-Kikorongo/Buranga, respectively, and similarly results of isotope analysis for these areas are in Tables 5 and 6. Relatively detailed analyses were carried out on samples from Kibiro, but only a few chemical components were analysed in samples from the other two areas. The composition of the geothermal samples from Kibiro is very similar to that recorded by Ármannsson (1994). The groundwater samples were collected from different locations this time, but examples of the two types of groundwater reported by Ármannsson (1994) were observed, termed brackish (e.g. UG-99-09, UG-01-02) and dilute (e.g. UG-01-07, UG-01-08).

4.1. Stable isotopes of water, and recharge to the geothermal systems

Isotope ratios, especially $^2H/^1H$ (usually reported in delta notation as δ^2H, Craig, 1961a) tend to be conservative, and are good indicators of water origins and of flow, mixing and evaporation processes. The $^{18}O/^{16}O$ ratio or $\delta^{18}O$ is similarly useful for cold waters, but in geothermal systems exchange may take place during water/rock interaction, causing an oxygen isotope shift to higher delta values, especially where the water/rock ratio is low, i.e. when permeability is poor.

Table 1
Kibiro: sample site information

Site name	Location	Type	Sample ID	Date	Longitude	Latitude	Altitude
Kibiro 2	Kibiro	GTH	UG-99-01	18/11/99	031,15,34E	01,40,45N	675
Nyababiri 1	Nyababiri	GWD	UG-99-02	19/11/99	031,17,65E	01,37,45N	1101
Mahogota 1	Mahogota	GWB	UG-99-03	19/11/99	031,17,13E	01,36,19N	1132
Kijura 1	Kijura	GWB	UG-99-04	20/11/99	031,18,31E	01,37,70N	1131
Kiganja 1	Kiganja	GWB	UG-99-05	20/11/99	031,18,39E	01,38,34N	1131
Bombo 1	Bombo PS	GWB	UG-99-06	20/11/99	031,15,49E	01,34,24N	1048
Kisukuma 1	Kisukuma	SPR	UG-99-07	20/11/99	031,18,34E	01,35,84N	1058
R. Hoimo 1	Hoimo	SRI	UG-99-08	22/11/99	031,18,69E	01,35,47N	1038
Abogora 1	Abogora	GWB	UG-99-09	22/11/99	031,14,50E	01,35,40N	989
R.Wambabya-Br	Wambabya	SRI	UG-99-10	22/11/99	031,06,87E	01,31,80N	992
R.Waki Falls	Waki Falls	SRI	UG-01-01	13/02/01	031,21,48E	01,46,20N	644
Biiso 1	Biiso	GWB	UG-01-02	13/02/01	031,24,54E	01,45,28N	991
R.Waki-Br	Waki Br.	SRI	UG-01-03	13/02/01	031,22,35E	01,42,34N	999
Kyeramya 1	Kyeramya	GWB	UG-01-04	13/02/01	031,19,26E	01,38,51N	1080
Nyakimese 1	Nyakimese	GWD	UG-01-05	14/02/01	031,17,51E	01,37,44N	1055
Bukona1	Bukona	GWB	UG-01-06	13/02/01	031,16,30E	01,38,08N	1094
Nyabago 1	Nyabago	GWB	UG-01-07	16/02/01	031,18,28E	01,36,43N	1076
Nyakabale 1	Nyakabale	GWB	UG-01-08	17/02/01	031,19,13E	01,38,25N	1060
Kiryawanga 1	Kiryawanga	GWD	UG-01-09	15/02/01	031,19,45E	01,39,31N	1071
Kibiro 5	Kibiro	GTH	UG-01-10	10/05/01	031,15,34E	01,40,45N	644
Kibiro 14	Kibiro	GTH	UG-01-11	10/05/01	031,15,37E	01,40,55N	641
Albert 1	Albert	SLA	UG-01-12	10/05/01	031,15,17E	01,41,14N	625
Albert 2	Albert	SLA	UG-01-13	10/05/01	031,15,19E	01,41,14N	624
Kisonde1	Kisonde	GWB	UG-01-18	18/12/01	031,21,23E	01,31,56N	1182
R.Muhu-Br	R.Muhu	SRI	UG-01-19	18/12/01	031,21,47E	01,32,47N	1160
R.Rwempanga-Br	R.Rwempanga	SRI	UG-01-20	18/12/01	031,24,58E	01,34,30N	1122
R.Siba-Br	R.Siba	SRI	UG-01-21	18/12/01	031,29,38E	01,40,19N	1151
R.Kabarongo Br.	R.Kabarongo	SRI	UG-01-22	18/12/01	031,26,37E	01,36,28N	1151
Iseisa 1	Iseisa	GWD	UG-01-23	18/12/01	031,16,24E	01,32,25N	1071
Kapapi 1	Kapapi	GWB	UG-01-24	19/12/01	031,21,43E	01,41,40N	1036
Karongo 1	Karongo	GWB	UG-01-25	19/12/01	031,18,27E	01,28,55N	1110
Kibanda 1	Kibanda	GWB	UG-01-26	20/12/01	031,18,20E	01,39,25N	1047
Bwikya 1	Bwikya	GWB	UG-01-27	20/12/01	031,17,12E	01,34,48N	1085
R.Kachururu	Kachururu	SRI	UG-01-28	20/12/01	031,16,24E	01,37,38N	1033
Bukerenge 1	Bukerenge PS	GWB	UG-01-29	20/12/01	031,14,49E	01,30,28N	1100

GTH: geothermal spring; GWD: groundwater from dug well; GWB: groundwater from borehole; SPR: cold water spring; SRI: stream or river water; SLA: lake water. Latitude and longitude are given in degrees, minutes and seconds.

A general worldwide relationship between δ^2H and δ^{18}O has been established (Craig, 1961b) as the Global Meteoric Water Line (GMWL):

$$\delta^2\mathrm{H} = 8^*\delta^{18}\mathrm{O} + 10 \tag{1}$$

Similarly, the observed local meteoric line (LMWL) for precipitation at Entebbe (GNIP, 1999) has the same slope but higher deuterium excess with the equation:

$$\delta^2\mathrm{H} = 8^*\delta^{18}\mathrm{O} + 12.3 \tag{2}$$

Table 2
Katwe-Kikorongo, Buranga: sample site information

Area	Site name	Location	Type	Sample ID	Date	Longitude	Latitude	Altitude
Katwe-Kikorongo	L.Kitagata 2	L.Kitagata	GTH	UG-02-01	14/03/02	029,58,14E	00,03,48S	944
	L.Kitagata 5	L.Kitagata	GTH	UG-02-02	14/03/02	029,58,14E	00,03,48S	944
	L.Kitagata-lw	L.Kitagata	SLA	UG-02-03	14/03/02	029,58,46E	00,03,47S	943
	L.Katwe 4	L.Katwe	GWS	UG-02-04	14/03/02	029,52,50E	00,07,21S	906
	L.Katwe13	L.Katwe	GWS	UG-02-05	14/03/02	029,51,33E	00,07,40S	912
	R.Nyamugasani 1	R.Nyamugasani	SRI	UG-02-06	15/03/02	029,50,35E	00,07,25S	942
	R.Kanyambara 1	R.Kanyambara	SRI	UG-02-07	15/03/02	029,52,13E	00,00,12N	1031
	R.Nyamugasani 2	R.Nyamugasani	SRI	UG-02-08	15/03/02	029,53,57E	00,00,32N	1054
	L.Kikorongo 1	L.Kikorongo	SLA	UG-02-09	15/03/02	030,00,45E	00,00,43S	928
	L.Kasenyi 1	L.Kasenyi	GWS	UG-02-10	15/03/02	030,07,35E	00,02,24S	908
Buranga	Kagoro 20	Kagoro	GTH	UG-02-12	16/03/02	030,09,41E	00,49,53N	704
	Nyansimbe 1	Nyansimbe	GTH	UG-02-13	16/03/02	030,09,48E	00,49,57N	683
	Mumbuga 5	Mumbuga	GTH	UG-02-14	16/03/02	030,09,50E	00,49,59N	684
	R.Mungera 1	R.Mungera	SRI	UG-02-15	16/03/02	030,09,58E	00,49,49N	698
	R.Nkisya 1	R.Nkisya	SRI	UG-02-16	16/03/02	030,08,49E	00,48,28N	712
	R.Kirimia-Br	R.Kirimia	SRI	UG-02-17	16/03/02	030,05,44E	00,47,44N	728
	R.Sempaya 1	R.Sempaya	SRI	UG-02-18	17/03/02	030,10,26E	00,50,50N	710
	R.Semuliki-BK	R.Semuliki	SRI	UG-02-19	17/03/02	030,09,27E	00,53,04N	658
	R.Nyambiga-Br	R.Nyambiga	SRI	UG-02-20	17/03/02	030,12,34E	00,50,07N	1152
	R.Katojo-Br	R.Katojo	SRI	UG-02-21	17/03/02	030,13,35E	00,50,10N	1056
	R.Nyabushokoma-Br	R.Nyabushokoma	SRI	UG-02-22	17/03/02	030,13,59E	00,48,25N	1012
	R.Wasa-Br	R.Wasa	SRI	UG-02-23	18/03/02	030,11,11E	00,43,03N	1613
	R.Wasa 1	R.Wasa	SRI	UG-02-24	18/03/02	030,14,41E	00,47,12N	984

GTH: geothermal spring; GWD: groundwater from dug well; GWB: groundwater from borehole; SPR: cold water spring; SRI: stream or river water; SLA: lake water. Latitude and longitude are given in degrees, minutes and seconds.

Table 3
Kibiro: analytical results (mg/l), except for pH and EC (electrical conductivity, in μS/cm at 25 °C)

Sample ID	pH	T (°C)	EC	TDS	Na	K	Mg	Ca	Sr	Cl	SO_4	SiO_2
UG-99-02	7.13	22.0	276	164	16.9	1.6	11.5	22.5		4.3	32.0	53.6
UG-99-03	6.27	22.0	122	70	6.8	1.9	3.1	8.4		1.3	2.2	47.0
UG-99-04	8.10	22.0	183	112	10.7	2.0	8.1	13.5		5.0	1.5	47.0
UG-99-05	7.31	22.0	154	91						7.5		60.5
UG-99-06	6.62	22.0	143	87	7.1	1.9	4.2	13.5		1.8	2.3	37.5
UG-99-07	7.37	23.0	27	18						2.5		53.0
UG-99-08	7.33	19.0	41	26						0.0		16.1
UG-99-09	7.60	23.0	718	328	29.0	6.7	35.6	29.8		54.0	99.0	41.0
UG-99-10	7.50	19.0	70	40						10.0		20.7
UG-01-01	7.61	21.0	78	37	5.4	1.7	3.1	5.5		2.3	2.8	18.7
UG-01-02	6.90	24.0	565	276								
UG-01-03	7.45	20.0	74	35	4.5	1.6	2.7	8.5		2.6	2.5	18.5
UG-01-04	6.51	23.0	176	84	8.5	1.7	6.5	11.5		6.9	11.5	46.7
UG-01-05	7.00	23.0	167	80	13.1	2.4	6.1	9.5		7.1	11.0	59.7
UG-01-06	7.03	21.0	109	52								
UG-01-07	6.03	22.0	35	16	4.8	1.8	0.6	1.0		2.7	0.5	13.7
UG-01-08	6.28	22.0	75	35	9.2	4.1	1.1	2.7		2.8	7.3	40.3
UG-01-09	7.24	22.0	268	129								
UG-01-10	7.42	86.0	8700	4770	1470	180	9.6	94.0	0.68	2780	4.5	147
UG-01-11	7.49	77.0	7860	4240	1490	192	9.6	96.0	3.00	2760	1.9	126
UG-01-12		28.0										
UG-01-13		28.0										
UG-01-18	6.60	22.0	193		12.3	2.1	7.1	10.8	0.16	3.0	9.2	42.0
UG-01-19	7.34	21.0	59		5.6	1.7	2.4	3.5		1.5	3.0	6.2
UG-01-20	7.21	17.0	50		4.5	1.7	1.6	2.6	0.03	4.1	3.5	17.1
UG-01-21	7.22	19.0	78		5.1	1.2	2.8	5.4		1.5	2.5	21.3
UG-01-22	7.30	18.0	66		4.2	1.5	1.6	5.8		2.8	3.1	17.2
UG-01-23	5.24	20.0	33		2.7	1.1	0.6	2.0	0.01	1.6	2.7	10.8
UG-01-24	6.56	23.0	382		39.0	3.3	8.9	18.5		8.5	58.0	69.1
UG-01-25	5.35	22.0	32		2.4	0.8	0.3	3.1		1.5	4.5	6.3
UG-01-26	7.33	23.0	635		34.0	4.8	17.5	64.0		11.5	110.0	63.0
UG-01-27	6.63	21.0	218		8.9	3.9	5.6	10.2	0.06	2.5	2.9	58.8
UG-01-28	6.84	19.0	174		12.3	0.8	6.5	11.5	0.10	1.5	2.1	23.1
UG-01-29	6.41	21.0	130		9.4	4.1	5.3	5.0	0.05	2.5	2.1	58.7

Table 4
Katwe-Kikorongo, Buranga: analytical results (mg/l), except for pH and EC (electrical conductivity, in μS/cm at 25 °C)

Area	Sample ID	pH	*T* (°C)	EC	Sr	HCO_3	H_2S
Katwe-Kikorongo	UG-02-01	8.61	57.0	33000	1.04	2680	
	UG-02-02	8.42	69.0	33300	2.40	2740	
	UG-02-03	9.98	28.0	221600	8.40		
	UG-02-04	9.90	27.0	48200	1.60	5710	31.5
	UG-02-05	7.78	25.0	387	0.28		
	UG-02-06	7.48	18.0	79	0.02		
	UG-02-07	7.32	18.0	106.2			
	UG-02-08	7.43	17.0	70.2			
	UG-02-09	9.78	29.0	8200			
	UG-02-10	7.92	29.0	2460			
Buranga	UG-02-12	8.02	92.0	21600	5.90	2630	
	UG-02-13	8.32	88.0	21600	1.80	2403	
	UG-02-14	8.12	96.0	19550	6.00	2183	
	UG-02-15	7.99	23.0	169.8	0.11		
	UG-02-16	7.93	23.0	303			
	UG-02-17	8.24	25.0	338			
	UG-02-18	8.29	25.0	522	0.11		
	UG-02-19	8.41	23.0	5420			
	UG-02-20	8.04	21.0	488			
	UG-02-21	8.25	24.0	305			
	UG-02-22	7.97	23.0	293			
	UG-02-23	8.00	15.0	223			
	UG-02-24	8.34	19.0	442			

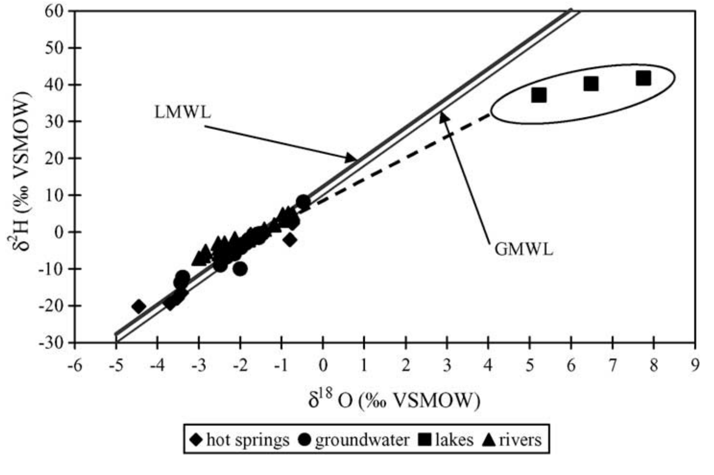

Fig. 6. Katwe-Kikorongo, Buranga and Kibiro: stable isotope compositions of hot and cold water samples.

Table 5
Kibiro geothermal area and surroundings: isotope data

Sample ID	δ^{18}O VSMOW	δ^{2}H VSMOW	Tritium TU	TU-2σ	^{13}C PDB	^{14}C PMC	δ^{34}S (SO_4)	δ^{18}O (SO_4)	$^{87/86}$Sr
UG-99-01	−2.05	−11.1	1.25	0.66	−14.1	119.12			
UG-99-02	−1.79	−2.4	1.65	0.7					
UG-99-03	−1.65	−0.95	1.88	0.68					
UG-99-04	−1.58	−0.9	0.81	0.62					
UG-99-05	−1.46	−0.35	1.17	0.68					
UG-99-06	−1.57	−0.5	0.92	0.64					
UG-99-07	−0.47	8.15	2.66	0.72					
UG-99-08	−0.84	5.1	3.2	0.76					
UG-99-09	−2.48	−8.95	1.36	0.7					
UG-99-10	−0.97	4.75	1.79	0.72					
UG-01-01	−0.74	4.6	2.49	0.42					
UG-01-02	−1.93	−3.3	1.04	0.38					
UG-01-03	−0.94	3.2	2.7	0.44					
UG-01-04	−1.67	−1.4	0.94	0.38					
UG-01-05	−1.7	−1.7	1.57	0.4					
UG-01-06	−1.98	−4.2	0.13	0.36					
UG-01-07	−1.66	−1.6	2.79	0.44					
UG-01-08	−1.55	−1.5	1.25	0.38					
UG-01-09	−1.84	−2.8	0.92	0.38					
UG-01-10							12.7	12.4	0.7322
UG-01-11							24.2	15.5	0.7321
UG-01-12	5.22	37.1							
UG-01-13	5.23	37.2							
UG-01-18	−1.7	−1.6	1.4	1.2					0.7179
UG-01-19	−1.75	−0.6	3	1.2					
UG-01-20	−1.8	−1.2	1	0.7					0.7165
UG-01-21	−1.18	2	2.4	0.7					
UG-01-22	−1.42	0.8	2.8	0.7					
UG-01-23	−1.58	−1.4	3.5	0.7					0.7140
UG-01-24	−2.14	−5.9	2.2	0.7					
UG-01-25	−1.86	−3	2.3	0.7					
UG-01-26	−2.33	−6.8	1.4	0.7					
UG-01-27	−1.8	−2.1	1.3	0.7					0.7512
UG-01-28	−0.73	5	2.3	0.7					0.7241
UG-01-29	−1.52	−0.4	1.5	0.7					0.7370

Notes: VSMOW, Vienna Standard Mean Oceanic Water; TU, tritium units; PDB, Pee Dee belemnite; PMC, percent modern carbon.

Table 6
Katwe-Kikorongo, Buranga: isotope data (VSMOW, Vienna Standard Mean Ocean Water; TU, tritium units)

Area	Sample ID	δ^{18}O‰ VSMOW	δ^{2}H‰ VSMOW	Tritium TU	TU-2σ	δ^{34}S (SO_4) CDT	δ^{18}O (SO_4) VSMOW	$^{87/86}$Sr
Katwe-Kikorongo	UG-02-01	−0.74	2.4	<0.3		9.6	14.1	0.7060
	UG-02-02	−0.80	−2.1	<0.2		9.6	13.1	0.7060
	UG-02-03	7.76	41.8	1.6	0.4			0.7068
	UG-02-04	−2.00	−10.0	<0.3		33.0	26.6	0.7070
	UG-02-05	−3.39	−12.3	<0.4				0.7062
	UG-02-06	−2.84	−5.2	2.2	0.6			0.7171
	UG-02-07	−2.54	−3.1	2.1	0.4			
	UG-02-08	−3.00	−7.1	2.1	0.4			
	UG-02-09	6.49	40.2	1.9	0.4			
	UG-02-10	−3.44	−13.7	<0.2				
Buranga	UG-02-12	−3.70	−19.4	<0.2		7.6	6.3	0.7196
	UG-02-13	−3.53	−18.0	<0.2		7.2	6.6	0.7196
	UG-02-14	−3.42	−16.5	<0.2		6.3	5.3	0.7195
	UG-02-15	−2.11	−4.0	2.1	0.4			0.7247
	UG-02-16	−2.44	−4.2	2.3	0.6			
	UG-02-17	−2.38	−3.0	2.0	0.4			
	UG-02-18	−2.14	−1.8	1.8	0.8			0.7287
	UG-02-19	−1.81	−2.1	2.5	1			
	UG-02-20	−2.51	−5.9	1.9	0.8			
	UG-02-21	−2.39	−4.4	2.7	1			
	UG-02-22	−2.18	−3.3	2.4	1			
	UG-02-23	−2.89	−6.4	3.4	1			
	UG-02-24	−2.51	−4.4	2.6	1.2			

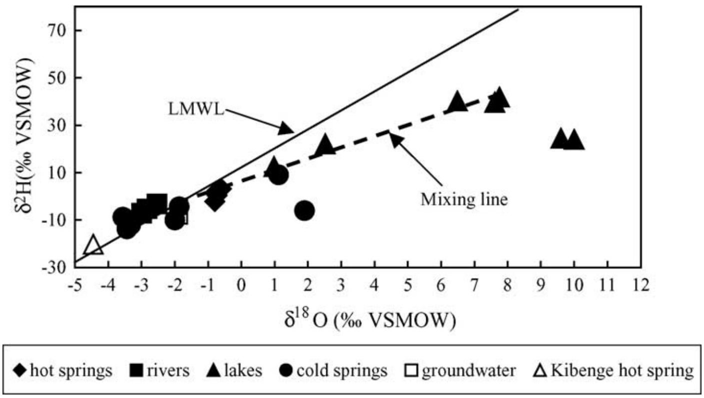

Fig. 7. Katwe-Kikorongo: stable isotope compositions of hot and cold water samples.

Both lines have been drawn in Fig. 6 and the stable isotope results for waters from the three areas plotted. All hot spring waters, groundwaters, and river waters plot close to the two lines. The thermal waters show isotopic compositions compatible with the LMWL, confirming the meteoric origin of the water circulating in the geothermal systems. The lake waters (enclosed in an oval) are higher in δ^2H and δ^{18}O as a result of evaporation, as shown by the dotted trend line, which represents a typical evaporation line.

In the Katwe-Kikorongo area (Fig. 7) there are signs of both oxygen and deuterium shifts of the hot spring waters from the potential source water, which results from slight mixing with lake water. The lake waters have been affected by strong evaporation, resulting in increased δ^2H and δ^{18}O. The Katwe-Kikorongo hot spring water is probably a mixture of water similar to the most depleted local groundwaters and water from lakes in the area. The mixing model for Katwe is also represented in the same diagram (Fig. 7) by a dashed line. This model indicates that the geothermal water is a mixture of the hot water component with the lake water.

In the Buranga area (Fig. 8) there are no signs of an oxygen shift from the LMWL for hot spring waters, an indication of reasonably high permeability. All the cold waters (rivers) are more enriched in δ^2H than the hot spring waters by about 5‰, an indication that these cold waters cannot be a source of recharge for the thermal waters in this area. The diagram also shows the plot of the Kibenge geothermal area in the bottom left-hand corner, above the LMWL. As in the Katwe-Kikorongo area, the source of recharge for Buranga is represented by water similar to the Kibenge hot spring although it is unlikely to provide the recharge for both areas considering its location and elevation.

In the Kibiro area (Fig. 9), there is an insignificant oxygen shift in the hot spring waters from the LMWL. This could result from limited water–rock interaction with no change in δ^{18}O of water or rock, from old age, or from a high water–rock ratio with rock δ^{18}O changed to equilibrate with water. The groundwaters that could be the source of recharge for this area are represented by Kapapi (UG-01-24), Kibanda (UG-01-26), Ndalagi (UG-93-26) and Bukona (UG-01-06), all located east and southeast of Kibiro (Fig. 5). A similar source located south of Kibiro, represented by the Abogora borehole (UG-99-09), has also

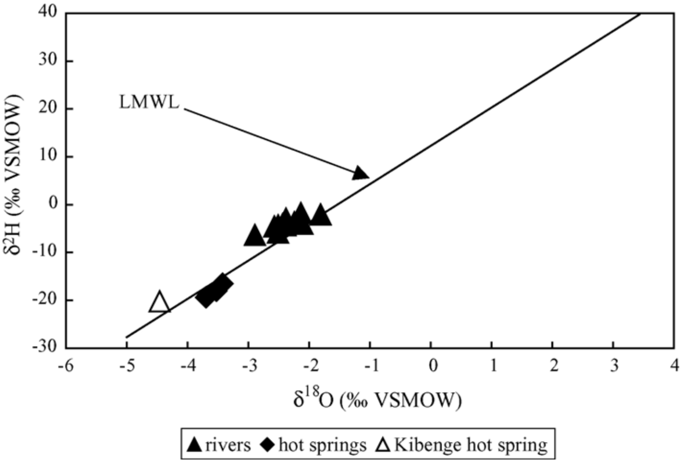

Fig. 8. Buranga: stable isotope compositions of hot and cold water samples.

been suggested as a candidate for recharge to this area (Kato, 2000). The Abogora area is connected to Kibiro by a fault along which the river Kachururu flows, although isotope results do not indicate possible recharge from this river. The Wantembo borehole (UG-93-24), located further northeast of Kibiro, is the most depleted cold water sampled in the surrounding areas that could represent a source of recharge to Kibiro from high ground. All the river waters are more enriched in δ^2H than the hot spring waters, an indication that they cannot be the source of recharge for the thermal waters. The lake water is highly evaporated and most likely is not a source of recharge for Kibiro.

Katwe-Kikorongo and Buranga geothermal areas are most likely recharged from high ground in the Rwenzori Mountains. The source of the recharge is similar to that of the

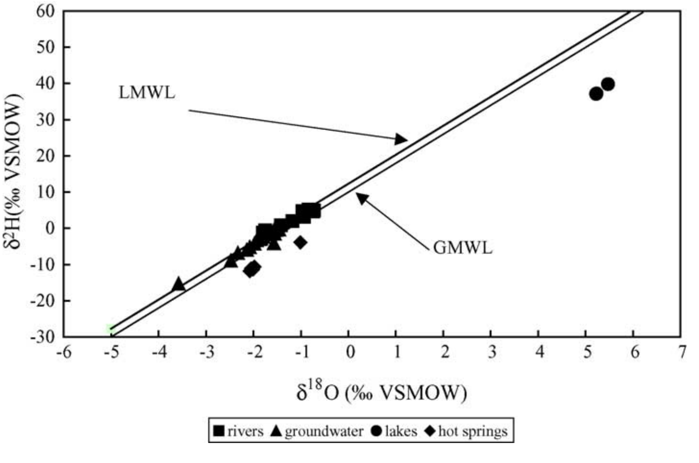

Fig. 9. Kibiro: stable isotope compositions of hot and cold water samples.

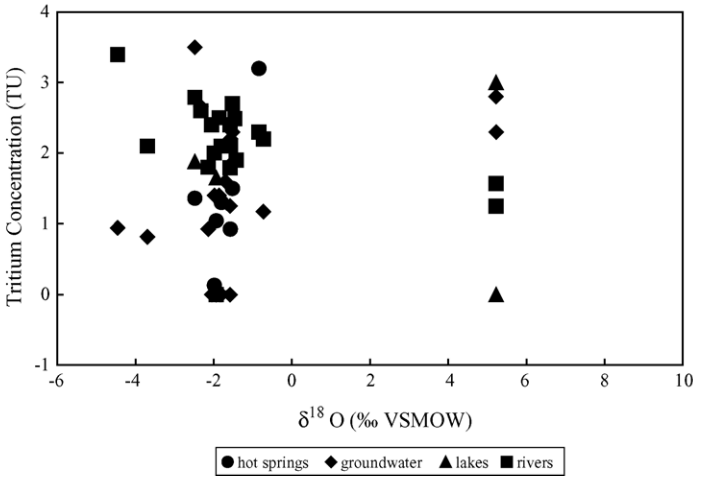

Fig. 10. Katwe-Kikorongo, Buranga and Kibiro: histogram of tritium content in water samples.

Kibenge geothermal area. This area is located at the foot of the Rwenzori Mountains and the recharge most likely comes from there. The Katwe-Kikorongo hot spring water is probably a mixture of this high-elevation component, local ground water (Katwe cold springs) and water from lakes in the area.

The Rwenzori Mountains are snow-capped and characterized by a number of lakes at high elevation that are recharged from snowmelt. It is possible that some of these lakes are losing water through fractures (faults) that connect with the Katwe-Kikorongo and Buranga geothermal reservoirs. The evidence for this is the earthquakes that simultaneously affect Bundibugyo and Kabarole districts, indicating that the two places are connected by one or more faults, possibly passing under the Rwenzori Mountains. Kabarole and Bundibugyo districts are situated east and west of the northern part of these mountains, respectively.

The Kibiro hot spring water is either recharged from the areas above the Rift escarpment located east and southeast and closer to the geothermal area or from a higher elevation than all the cold-water sampling points. This water is likely to be channeled through faults that have been identified in the area oblique to the eastern escarpment of the Rift Valley under which Kibiro lies. The only higher ground close by is the Mukihani-Waisembe Ridge in Kitoba sub-county, located 20 km southeast of Kibiro, but the mechanism by which meteoric water from this area may reach the geothermal area has yet to be established.

4.2. Tritium and possible mixing processes

Tritium (^3H) analyses (Fig. 10) indicate that river waters are much higher in tritium content than groundwaters and lake waters and that there is no tritium in hot spring waters from the Katwe-Kikorongo and Buranga areas. The Kibiro hot spring water plots with the groundwaters, which indicates that the thermal water has some cold groundwater contribution and is therefore a mixture of hot and cooler waters. The diagram also shows that the Katwe-Kikorongo and Buranga hot spring waters have a residence time of more than 50

Table 7
Chemical and isotope geothermometer temperatures (°C)

Area	Site	T_{qz}[a]	T_{KMg}[b]	T_{NaK}[c]	T_{NaKCa}[d]	$T_{S^{18}O_4H_2{}^{18}O}$[e]
Kibiro	Kibiro 5	160	148	217	220	137
	Kibiro 14	151	150	222	223	110
Katwe-Kikorongo	L.Kitagata 2	116[f]		145[f]		130
	L.Kitagata 5	134[f]		162[f]		140
Buranga	Kagoro 20	122[f]		111[f]		188
	Nyansimbe 17	104[f]		113[f]		189
	Mumbuga 5	117[f]		111[f]		212

[a] Fournier and Potter (1982).
[b] Giggenbach (1988).
[c] Arnórsson et al. (1983).
[d] Fournier and Truesdell (1973).
[e] Mizutani and Rafter (1969).
[f] Results from Ármannsson (1994).

years. It should be noted, however, that as the tritium background in the precipitation for the area is rather low, up to a few tritium units only, indications of mixing may not always be clear.

4.3. Isotope and chemical geothermometry

The results of the geothermometer temperature calculations are presented in Table 7. Four types of chemical geothermometer temperatures were obtained for the Kibiro samples, as well as the sulfate-water ($S^{18}O_4$–$H_2{}^{18}O$) isotope geothermometer temperature, which is well established for water-dominated fields (Lloyd, 1968; Mizutani and Rafter, 1969; McKenzie and Truesdell, 1977). A plot of $\delta^{18}O$ in H_2O versus $\delta^{18}O$ in SO_4 for the hot spring waters in the three areas is presented in Fig. 11.

Ármannsson (1994) found that indicated geothermometer temperatures for samples from Kibiro fell into two groups, one about 150 °C and another in the 200–220 °C range. Lower temperatures were indicated by single-component solute geothermometers (e.g. quartz) and by geothermometers based on ratios of components that equilibrate rapidly (e.g. K–Mg). Higher temperatures were indicated by geothermometers based on ratios between components that equilibrate more slowly (e.g. Na–K and gas geothermometers). Mixing with cooler groundwaters may have affected the SiO_2 and K–Mg geothermometer temperatures. The use of mixing models (SiO_2-enthalpy, SiO_2–CO_2) and the construction of log(Q/K) diagrams supported this explanation.

A substantial part of the groundwater component that mixes with the geothermal component must be the brackish type that was found in some of the boreholes in the vicinity. One characteristic of this brackish water is a relatively high sulfate concentration. Two samples of such a water reported by Ármannsson (1994) had sulfate concentrations of 139 and 227 mg/l, and sample UG-99-09 reported in this study had 99 mg/l (Table 3). The sulfate concentrations of the geothermal samples obtained by Ármannsson (1994) were substantially lower (15.4–49.9 mg/l), and those obtained in the present study even

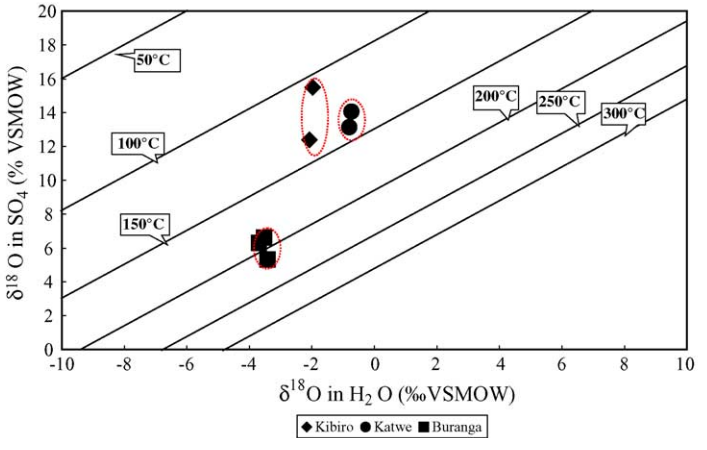

Fig. 11. Katwe-Kikorongo, Buranga and Kibiro: oxygen isotope geothermometer temperatures based on the $\delta^{18}O$ in SO_4–H_2O pairs.

lower (1.9 and 4.5 mg/l, Table 3). Thus, most of the sulfate in the geothermal samples is expected to originate from the groundwater component whose presence is confirmed by the results for tritium (see above). Exchange of oxygen isotopes between dissolved sulfate and water is exceedingly slow in neutral and alkaline solutions below 200 °C (McKenzie and Truesdell, 1977), so equilibrium is probably not reached for the mixed solution and the $S^{18}O_4$–$H_2{}^{18}O$ temperatures are probably too low (Table 7, Fig. 11). Therefore, the model suggesting a reservoir temperature in excess of 200 °C still seems valid for Kibiro.

Solute geothermometers were a little difficult to use in Katwe-Kikorongo because of the extreme salinity of the thermal fluid. The sulfate concentrations are relatively high and all indications suggest that the geothermal system is relatively old. Thus, conditions for sulfur isotope determination and attainment of isotope equilibrium are good and the results compare reasonably well with those of the solute geothermometers (Table 7). Some indications of possible mixing with groundwater were inferred from log(Q/K) diagrams (Ármannsson, 1994), but the results for tritium do not bear this out. In this case, however, it would be the geothermal component that supplied most of the sulfate. A subsurface temperature of 130–140 °C is therefore predicted for Katwe-Kikorongo on the basis of geothermometric data.

In the earlier study by Ármannsson (1994) a good agreement was obtained for all solute geothermometers tested for several hot springs and pools in Buranga and it was concluded that the subsurface temperature was 120–130 °C. Log(Q/K) diagrams suggest about 135 °C and there are few indications of mixing with groundwater. A gas geothermometer temperature based on the CH_4/C_2H_6 ratio (Darling et al., 1995) gave a higher temperature of 164 °C, but H_2 was not detected in the gas, so the temperature of the system is likely to be well below 200 °C. The present results reveal values from 188–212 °C, which seem higher than could be expected. There are two possible explanations. As no solute geothermometer results exist for the present samples it is possible that changes have taken place and that

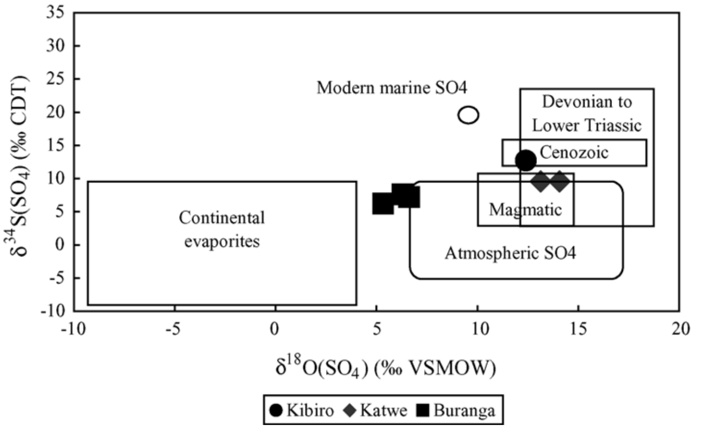

Fig. 12. Katwe-Kikorongo, Buranga and Kibiro: ranges of $\delta^{34}S$ and $\delta^{18}O$ values of sulfates of various origins in groundwater.

the system is hotter now than in 1993. This must be regarded as unlikely but might be connected to the February 1994 earthquake (Mbojana, 1994) that certainly changed the surface manifestations in the area.

A more plausible explanation is that the Buranga geothermal system was hotter in the past and that the relative slowness of the exchange of oxygen isotopes between dissolved sulfate and water (McKenzie and Truesdell, 1977) has caused the geothermometer to "remember" an older and higher temperature. The breakdown of C_{2+} hydrocarbons, which is the basis for the CH_4/C_2H_6 geothermometer, is also slowed down at temperatures around 150 °C so that the temperature of 164 °C recorded by this geothermometer could also be an older, "remembered" temperature. The most reasonable interpretation seems to be that the reservoir temperature at Buranga is now 120–130 °C, but that higher temperatures may have prevailed there in the past.

4.4. Sulfur isotopes and source of solutes

The isotopic composition of sulfur and oxygen in sulfates helps to differentiate between marine, evaporitic and volcanic sources of dissolved sulfate (Krouse, 1980; Pearson and Rightmire, 1980) and to determine its fate in the groundwater. The isotopic compositions expressed in $\delta^{34}S$ (SO_4) and $\delta^{18}O$ (SO_4) are important characteristics when the origin of water and sulfates is discussed. The variety of possible sources of dissolved sulfates, complex fractionation mechanisms, non-equilibrium state and uncertainties about the permeability of the groundwater systems, however, make the interpretation of the isotopic compositions of sulfate and bound oxygen a difficult task. Fig. 12 shows the ranges of $\delta^{34}S$ and $\delta^{18}O$ values for sulfates of various origins dissolved in groundwater (after Clark and Fritz, 1997). The hot spring waters from the three geothermal areas plot in different regions of the diagram. The figure shows that the source of sulfate for the Katwe-Kikorongo hot spring water is magmatic and hydrothermal, while

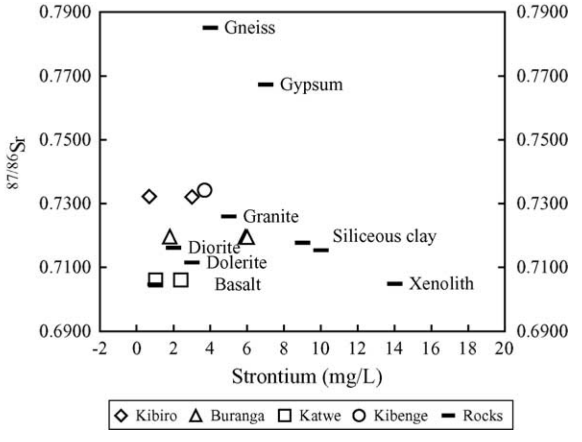

Fig. 13. Katwe-Kikorongo, Buranga and Kibiro: relationship between the $^{87/86}$Sr and Sr in geothermal waters, and corresponding values in rocks sampled from the same areas.

for Buranga it is from minerals or rocks (terrestrial evaporates), with a possible magmatic contribution, and for Kibiro it is from sediments, again with a possible magmatic contribution.

4.5. *Strontium isotopes ($^{87/86}Sr_{H_2O}$, $^{87/86}Sr_{Rock}$) and water–rock interactions*

A plot for hot water and rock samples from the three study areas (Fig. 13) indicates that $^{87/86}$Sr in most of the rocks is below 0.7400, with the exception of gypsum from Katwe and gneiss from Kibiro. This indicates that there is a possibility of water–rock interaction between these rocks and the geothermal fluids, which also plot below 0.7400. Fig. 13 also shows that geothermal waters from each of the individual areas are of identical strontium ratios ($^{87/86}Sr_{H_2O}$), but with varying strontium concentrations, which suggests a similar source of salinity for the thermal waters from a given area. A plot of strontium ratios in rocks on the same diagram indicates that the geothermal water most likely interacts with basalt (leucites and melilites) and ultramafic xenoliths in Katwe-Kikorongo, and with granitic gneisses in Buranga and Kibiro.

5. Conclusions

The waters recharging the hot springs in the three Ugandan geothermal areas under study come from higher elevations, most likely from the nearby Rwenzori Mountains in the case of Katwe-Kikorongo and Buranga. For Kibiro, the source is either from surrounding areas located east of Kibiro or from a higher elevation represented by the Mukihani-Waisembe ridge in Kitoba sub-county, southeast of Kibiro.

Subsurface temperatures predicted by isotope geothermometry are highest for Buranga (200 °C), but these may be older temperatures in a cooling system that is probably now at 120–130 °C. Lower temperatures are predicted for Katwe-Kikorongo (130–140 °C) and Kibiro (110–135 °C) The Kibiro data probably reflect low temperatures resulting from a mixing with relatively sulfate-rich groundwater and thus do not conflict with the model previously proposed for Kibiro (Ármannsson, 1994) in which a geothermal water of about 200 °C mixes with a brackish groundwater to produce a mixed water of about 150 °C. The Katwe results probably reflect a true subsurface temperature.

Reservoir rock types are most likely basalt (leucites and melilites) and ultramafic xenolith in Katwe-Kikorongo, and granitic gneisses in Buranga and Kibiro.

The major source of solutes in the waters of the three geothermal areas is rock dissolution, but some magmatic input is suggested.

Acknowledgements

The authors wish to thank the Government of Uganda and the International Atomic Energy Agency for their financial and material support for this study. Special thanks are due to the Uganda geothermal team members who participated in the collection of samples, and to the laboratories mentioned in the text that carried out the analyses.

References

Ármannsson, H., 1994. Geochemical Study on Three Geothermal Areas in West and Southwest Uganda. UNDDSMS UGA/92/002, unpublished report.

Arnórsson, S., Gunnlaugsson, E., Svavarsson, H., 1983. The chemistry of geothermal waters in Iceland. III. Chemical geothermometry in geothermal investigations. Geochim. Cosmochim. Acta 47, 567–577.

Craig, H., 1961a. Standard for reporting concentrations of deuterium and oxygen-18 in natural water. Science 133, 1833–1834.

Craig, H., 1961b. Isotopic variations in meteoric waters. Science 133, 1702–1708.

Clark, I.D., Fritz, P., 1997. Environmental Isotopes in Hydrology. Lewis Publishers, New York, pp. 328.

Darling, W.G., Griesshaber, E., Andrews, J.N., Ármannsson, H., O'Nions, R.K., 1995. The origin of hydrothermal and other gases in the Kenya Rift Valley. Geochim. Cosmochim. Acta 59, 2501–2512.

EASD, 1996. State of environment reporting in Uganda, Chapter 1. EASD, http://easd.org.za/soe/Uganda/soechapt1.htm.

EDICON, 1984. Aeromagnetic interpretation of Lake Albert/Edward portion of the Western Rift Valley, unpublished report, EDICON Inc., Denver, Colorado.

Fournier, R.O., Potter II, R.W., 1982. A revised and expanded silica (quartz) geothermometer. Geothermal Res. Council Bull. 11, 3–9.

Fournier, R.O., Truesdell, A.H., 1973. An empirical Na–K–Ca chemical geothermometer. Geochim. Cosmochim. Acta 37, 1255–1275.

Giggenbach, W.F., 1988. Geothermal solute equilibria. Derivation of Na–K–Mg–Ca geoindicators. Geochim. Cosmochim. Acta 32, 2749–2765.

Gíslason, G., Árnason, K., Eysteinsson, H., 2004. The Kibiro geothermal prospect. A Report on a Geophysical and Geological Survey. Prepared for the Icelandic International Development Agency and the Ministry of Energy and Mineral Development, Uganda, unpublished report, p. 109.

GNIP, 1999. Data from the Global Network for Isotopes in Precipitation (GNIP) since 1960. Site Entebbe (Airport), Uganda; latitude 0°,05′,0″N and longitude 32°,45′,0″E.

Kato, V., 2000. Geothermal field studies using stable isotope hydrology: case studies in Uganda and Iceland. UNUGTP-IAEA project UGA/08/003, Report 10, pp. 189–216.

Krouse, H.R., 1980. Sulfur isotopes in our environment. In: Fritz, P., Fontes, J.C. (Eds.), Handbook of Environmental Isotope Geochemistry. The Terrestrial Environment. Elsevier, Amsterdam, pp. 435–471.
Lloyd, R.M., 1968. Oxygen isotope behavior in the sulfate-water system. J. Geophys. Res. 73, 6099–6110.
Mbojana, S.A., 1994. Overview of Geothermal Exploration in Uganda. Geological Survey and Mines Department, Uganda, p. 16.
McKenzie, W.F., Truesdell, A.H., 1977. Geothermal reservoir temperatures estimated from the oxygen isotope compositions of dissolved sulfate and water from hot springs and shallow drillholes. Geothermics 5, 51–61.
Mizutani, Y., Rafter, T.A., 1969. Oxygen isotopic composition of sulfates. Part 3: Oxygen isotopic fractionation in the bisulfate ion-water system. N. Z. J. Sci. 12, 54.
Morley, C.K., Westcott, W.A., 1999. Sedimentary environments and geometry of sedimentary bodies determined from subsurface studies in East Africa. In: Morley, C.K. (Ed.), Geoscience of Rift Systems – Evolution of East Africa. AAPG Studies in Geology, pp. 211–231, No. 44.
Musisi, J., 1991. The Neogene geology of the Lake George-Edward basin, Uganda, Ph.D. thesis. Vrije Universiteit, Brussels.
Pearson Jr., F.J., Rightmire, C.T., 1980. Sulfur and oxygen isotopes in aqueous sulfur compounds. In: Fritz, P., Fontes, J.Ch. (Eds.), Handbook of Environmental Isotope Geochemistry. Elsevier, Amsterdam, pp. 227–258.